Voltage-dependent Gating Rearrangements in the Intracellular T1–T1 Interface of a K^+ Channel

Guangyu Wang and Manuel Covarrubias

Department of Pathology, Anatomy, and Cell Biology, Jefferson Medical College of Thomas Jefferson University, Philadelphia, PA 19107

The intracellular tetramerization domain (T1) of most eukaryotic voltage-gated potassium channels (Kv channels) exists as a "hanging gondola" below the transmembrane regions that directly control activation gating via the electromechanical coupling between the S4 voltage sensor and the main S6 gate. However, much less is known about the putative contribution of the T1 domain to Kv channel gating. This possibility is mechanistically intriguing because the T1–S1 linker connects the T1 domain to the voltage-sensing domain. Previously, we demonstrated that thiol-specific reagents inhibit Kv4.1 channels by reacting in a state-dependent manner with native Zn^{2+} site thiolate groups in the T1–T1 interface; therefore, we concluded that the T1–T1 interface is functionally active and not protected by Zn^{2+} (Wang, G., M. Shahidullah, C.A. Rocha, C. Strang, P.J. Pfaffinger, and M. Covarrubias. 2005. *J. Gen. Physiol.* 126:55–69). Here, we co-expressed Kv4.1 channels and auxiliary subunits (KChIP-1 and DPPX-S) to investigate the state and voltage dependence of the accessibility of MTSET to the three interfacial cysteines in the T1 domain. The results showed that the average MTSET modification rate constant (k_{MTSET}) is dramatically enhanced in the activated state relative to the resting and inactivated states (~260- and ~47-fold, respectively). Crucially, under three separate conditions that produce distinct activation profiles, k_{MTSET} is steeply voltage dependent in a manner that is precisely correlated with the peak conductance–voltage relations. These observations strongly suggest that Kv4 channel gating is tightly coupled to voltage-dependent accessibility changes of native T1 cysteines in the intersubunit Zn^{2+} site. Furthermore, cross-linking of cysteine pairs across the T1–T1 interface induced substantial inhibition of the channel, which supports the functionally dynamic role of T1 in channel gating. Therefore, we conclude that the complex voltage-dependent gating rearrangements of eukaryotic Kv channels are not limited to the membrane-spanning core but must include the intracellular T1–T1 interface. Oxidative stress in excitable tissues may perturb this interface to modulate Kv4 channel function.

The Journal of General Physiology

INTRODUCTION

Vital electrophysiological processes in the brain and heart depend on the precise orchestration of intramolecular motions in voltage-dependent K^+ channels (Kv channels). Current models of Kv channel activation gating propose that the opening of the main gate namely depends on the electromechanical coupling between segments S4 (voltage sensor) and S6 (activation gate), which are membrane-spanning regions of the Kv subunit (Yellen, 1998; Horn, 2000; Lu et al., 2002; Tristani-Firouzi et al., 2002; Bezanilla and Perozo, 2003; Long et al., 2005b). However, recent work has suggested the contribution of the intracellular NH_2-terminal tetramerization domain (T1) to activation gating (Cushman et al., 2000; Minor et al., 2000; Robinson and Deutsch, 2005; Wang et al., 2005), but there is no conclusive evidence for conformational coupling between the T1 domain and the voltage sensor.

The T1 domain of most eukaryotic Kv channels is responsible for the subfamily-specific assembly of Kv channel subunits (Li et al., 1992; Xu et al., 1995). It sits just below the voltage-sensing and pore-forming domains of the channel (Kobertz et al., 2000; Long et al., 2005a; Kim et al., 2004), and is connected to the transmembrane segments through the T1–S1 linker. Previous structure–function analyses of the Kv1 T1–T1 interface showed that the mutational perturbation of certain polar residues significantly affects voltage-dependent gating (Cushman et al., 2000; Minor et al., 2000; Robinson and Deutsch, 2005). Namely, these studies demonstrated that the mutations cause dramatic shifts in the voltage dependence of channel activation. For instance, the T46V mutation in the rat Kv1.2 channel stabilizes the closed state by destroying a buried hydrogen bond network between T46 and D79 in the T1–T1 interface without significantly changing the tertiary structure of the protein (Minor et al., 2000). In contrast, another T1 mutation (N136A) in the Aplysia Kv1.1 destabilizes the closed state and changes the tertiary structure near the central axis of the T1 tetramer (Cushman et al., 2000).

Recent crystallographic studies of the isolated Kv3 and Kv4 T1 domains revealed that the tetrameric

Correspondence to Manuel Covarrubias: manuel.covarrubias@jefferson.edu

The online version of this article includes supplemental material.

Abbreviations used in this paper: DTT, dithiothretiol; Kv, voltage-dependent potassium; MTSET, 2-trimethylammonium-ethyl-methanethiosulfonate bromide.

four-layer scaffold includes four C3H1 high-affinity Zn^{2+} sites in the T1–T1 intersubunit interface (Bixby et al., 1999; Nanao et al., 2003). Surprisingly, however, our recent studies showed that the Zn^{2+} site thiolate groups in Kv4 channels are not protected by Zn^{2+} against chemical modification and that the T1–T1 intersubunit interface may play a role in channel gating (Wang et al., 2005). We have hypothesized that the L4 layer at the membrane side of the T1 domain and the S6 gate may undergo conformational changes associated with voltage-dependent activation. To test the coupling between a putative T1 conformational change and voltage-dependent activation gating, we probed here the state-dependent accessibility changes of the unprotected Zn^{2+} site thiolate groups. Using thiol-specific reagents and patch-clamp electrophysiology combined with a concentration-clamp method, our experiments demonstrated a tight functional coupling between voltage-dependent gating and an apparent conformational change in the T1–T1 interface of the Kv4.1 channel. Moreover, cross-linking experiments supported the idea of a functionally critical and dynamic T1–T1 interface that contributes to channel gating. Altogether, these observations suggest strongly that the complex voltage-dependent gating rearrangements in eukaryotic Kv channels include coupled displacements involving the intracellular T1 domain. Therefore, the activation gating mechanism extends beyond the membrane-spanning core of the pore-forming subunits.

MATERIALS AND METHODS

Molecular Biology

Kv4.1 (mouse), DPPX-S (rat), and KChIP1 (rat) were maintained in pBluescript II KS, pSG5 (Stratagene), and a modified pBluescript vector, pBJ/KSM, respectively. DPPX-S and KChIP1 are gifts from B. Rudy (New York University, New York, NY) and Mark Bowlby (Wyeth-Ayerst Research, Princeton, NJ), respectively. Eight Kv4.1 mutants were used in this study (Table I and Fig. 3). All mutations were created using the QuickChange site-directed mutagenesis (Stratagene) and confirmed by automated sequencing (Kimnel Cancer Institute of Thomas Jefferson University). The capped cRNAs for expression in *Xenopus laevis* oocytes were synthesized using the mMessage mMachine kit for in vitro transcription (Ambion).

Heterologous Expression and Electrophysiology

Kv4.1 wild-type and mutant channels were coexpressed along with two auxiliary subunits (KChIP1 and DPPX-S) as described previously (Wang et al., 2005). The expression of the Kv4.1 ternary complex was necessary because mutations in the putative Zn^{2+} site yielded nonfunctional channels or inhibited expression profoundly. Our previous paper and an earlier study from the Pfaffinger laboratory showed that the apparently lethal phenotype of Zn^{2+} site mutants can be corrected by coexpression of the channels with KChIPs (Kunjilwar et al., 2004; Wang et al., 2005); and we have found that DPPX-S boosts the expression of the channels even further (Wang et al., 2005), which made possible the recordings from inside-out macropatches.

All currents were recorded using an Axopatch 200A amplifier (Axon Instruments). To probe the gating state-dependent accessibility of the thiolate groups of the T1 domain, the membrane-impermeant thiol-specific reagent MTSET (2-trimethylammonium-ethyl-methane-thiosulfonate bromide; Toronto Chemicals) (200–400 μM) was applied to the intracellular side of inside-out macropatches at various membrane potentials (see online supplemental material, available at http://www.jgp.org/cgi/content/full/jgp.200509442/DC1). The composition of the solution in the patch electrodes was (in mM) 96 NaCl, 2 KCl, 1.8 $CaCl_2$, 1 $MgCl_2$, and 5 HEPES (pH 7.4, adjusted with NaOH), and that of the bath solution was (in mM) 98 KCl, 0.5 $MgCl_2$, 1 EGTA, 10 HEPES (pH 7.2, adjusted with KOH). The tip resistance of the borosilicate patch pipette was typically 1–2 MΩ. An online P/4 procedure was applied to subtract the passive leak current and capacitive transients. The currents were filtered at 1–5 kHz and digitized at 5–100 kHz. All recordings were obtained at room temperature (23 ± 1°C).

For disulfide cross-linking experiments, we used a mild oxidizing solution containing 50 μM CuSO4 and 200 μM 1,10 *o*-phenanthroline (Cu/P) (Liu et al., 1996). To promote the formation of the disulfide bond between various cysteine pairs in the T1–T1 interface, the cytoplasmic side of the inside-out patches was treated for ∼5 min with fresh Cu/P. After Cu/P washout, 10 mM dithiothretiol (DTT) was used to reduce the disulfide bond (pH 8.6) (Wang et al., 2005), and 400 μM MTSET was employed to test for the presence of free thiolate groups. All chemicals for these experiments were purchased from Sigma-Aldrich.

Data Acquisition and Analysis

Voltage-clamp protocols and data acquisition were controlled by a Pentium-III class desktop computer interfaced to a 12 bit A/D converter (Digidata 1200 using Clampex 8.0; Axon Instruments). Clampfit 8.0 (Axon Instruments) and Origin 7.0 (Origin Lab Inc.) were used for data reduction and analysis. To determine the MTSET modification rate constant, the peak currents were plotted as a function of the cumulative time of exposure to MTSET. The time constant (τ) was computed from the best-fit exponential describing the time course of inhibition by MTSET, and the second-order rate constant k_{MTSET} was determined from this relationship: $k_{MTSET} = (1/\tau\ [MTSET])$. Data from at least three patches for each measurement are presented as mean ± SEM. The Student's *t* test (unpaired) was used to evaluate statistically significant differences between two groups of data.

Sources of Error

To test whether or not a mutant was inhibited by MTSET, we used continuous intracellular application of the reagent while the current was evoked by a 250-ms step depolarization to +80 mV from a holding potential of −100 mV (3 s, start-to-start) (Wang et al., 2005). The rate constants determined from these experiments were slow and similar to those obtained from measurements in the resting state (Figs. 1 and 2). This similarity is expected because even during continuous application, the channels spend most of the time in the resting state at −100 mV. In general, however, the measurement of very slow MTSET modification rate constants ($<50\ M^{-1}s^{-1}$) in the resting state was less accurate. This difficulty resulted from the limited survival of some inside-out patches, which did not always allow the modification to reach steady state. Under continuous application, steady state was reached typically in ∼4–5 min. To minimize the error, the constant term of the exponential function (see above) was fixed by assuming the value obtained from those experiments that were long and stable enough to reach steady-state. For wild-type and the mutants C11xA, C12xA, and C13xA, the fractional steady-state level of the inhibition by MTSET ranged approximately between 0.1 and 0.3 (Wang et al., 2005). The slow

TABLE I

Rate Constants of Kv4.1 Channel Modification by MTSET ($mM^{-1}s^{-1}$)

Kv4.1 channel	110	131	132	Cys/α subunit	Resting state	Inactivated state	Activated state
Wild-type (WT)	C	C	C	14	0.079 ± 0.019 $n = 6$	0.291 ± 0.044 $n = 3$	30.8 ± 4.2 $n = 5$
C11xA	C	C	C	3	0.092 ± 0.007 $n = 5$	0.330 ± 0.053 $n = 4$	21.2 ± 2.8 $n = 5$
WT+DPPX+KCHIP1	C	C	C	14	0.059 ± 0.005 $n = 4$	0.271 ± 0.027 $n = 4$	35.3 ± 7.9 $n = 4$
C11xA+DPPX+KCHIP1	C	C	C	3	0.038 ± 0.003 $n = 3$	0.328 ± 0.028 $n = 6$	19.0 ± 3.2 $n = 6$
C12xA+DPPX+KCHIP1	A	C	C	2	0.078 ± 0.004[b] $n = 5$	0.280 ± 0.034 $n = 5$	13.8 ± 2.0 $n = 5$
C13xA+DPPX+KCHIP1	C	A	A	1	0.050 ± 0.007 $n = 6$	0.212 ± 0.037[c] $n = 5$	6.81 ± 0.73[a] $n = 3$
C14xA+DPPX+KCHIP1	A	A	A	0	No effect $n = 3$	No effect $n = 4$	No effect $n = 4$

All mutants of Kv4.1 channel contain the following additional substitutions: C[105, 257, 322, 392, 467, 484, 490, 532, 533, 589, 642]A. The tabulated Cys/α subunit are intracellular.

[a]Difference against corresponding C11xA and C12xA is statistically significant at $P < 0.01$.

[b]Difference against corresponding C11xA is statistically significant at $P < 0.01$.

[c]Difference against corresponding C11xA is statistically significant at $P = 0.03$.

rate constants in the resting state were not corrected for the possible loss of some reagent due to hydrolysis during the application period. At neutral pH, the half-life of MTSET is 10–11 min (Karlin and Akabas, 1998).

Online Supplemental Material

Rapid reagent application and verification of the switching and exchange processes were performed as described in the online supplemental materials (available at http://www.jgp.org/cgi/content/full/jgp.200509442/DC1).

RESULTS

Kv4.1 Cysteines in the T1 Interfacial Zn^{2+} Site Undergo State-dependent Modification by MTSET in the Presence of Auxiliary Subunits

To investigate the possible functional coupling between the transmembrane activation machinery and the T1 domain, all but three intracellular Zn^{2+} site cysteines in the T1–T1 interface of the Kv4.1-α subunit were mutated to alanines (Kv4.1-C11xA) (Table I); and the wild-type or mutant Kv4.1-α subunit was coexpressed with the Kv4 auxiliary subunits KChIP1 and DPPX-S (ternary complex) as shown previously (Wang et al., 2005). The functional impact of the remaining cysteines was probed upon chemical modification with a thiol-specific reagent. Fig. 1 shows that internal application of the membrane-impermeant MTSET irreversibly inhibits ternary complexes of wild-type or C11xA channels in the resting, activated, or inactivated state. In contrast, and regardless of the gating state of the channel, MTSET had no effect on the C14xA mutant, which has no remaining intracellular cysteines. More significantly, the rate of the inhibition of ternary C11xA was strongly gating state dependent (Fig. 2), which is in agreement with previously published results obtained in the absence of auxiliary subunits (Wang et al., 2005). When MTSET was applied to channels in the resting state (240 ms, at −120 mV), the time course of the inhibition was very slow ($k_{MTSET} = 0.038\ mM^{-1}s^{-1}$). In sharp contrast, when a 7-ms pulse of MTSET was applied immediately following current activation by a strong step depolarization to +80 mV, the rate constant of inhibition was ∼475-fold faster ($k_{MTSET} = 19\ mM^{-1}s^{-1}$). When a 120-ms pulse of MTSET was applied at the end of a long step depolarization to +80 mV to test the inactivated state (Fig. 1), the rate constant of inhibition by MTSET was intermediate ($k_{MTSET} = 0.33\ mM^{-1}s^{-1}$) between those for resting and activated channels. These observations confirm that the chemical modification of at least one thiolate group in the T1 interfacial Zn^{2+} site causes inhibition of the Kv4.1 channel, implying that these intersubunit interfaces play a critical functional role (Wang et al., 2005). Importantly, the state-dependent cysteine accessibility rate constants are correlated with the main functional states of the Kv4.1 channel. Thus, a dynamic T1–T1 interface could adopt three distinct conformations in resting, activated, and inactivated channels because the targeted intracellular cysteines in the C11xA mutant are all located in the interfacial Zn^{2+} site. These conformational correlatives are not induced by the eleven Cys→Ala mutations or the presence of auxiliary subunits because we observed similar state dependence and rate constants with wild-type and C11xA in the absence or presence of KChIP1 and DPPX-S (Table I).

To test whether the integrity of the T1 Zn^{2+} site and the number of cysteines in this site are important in

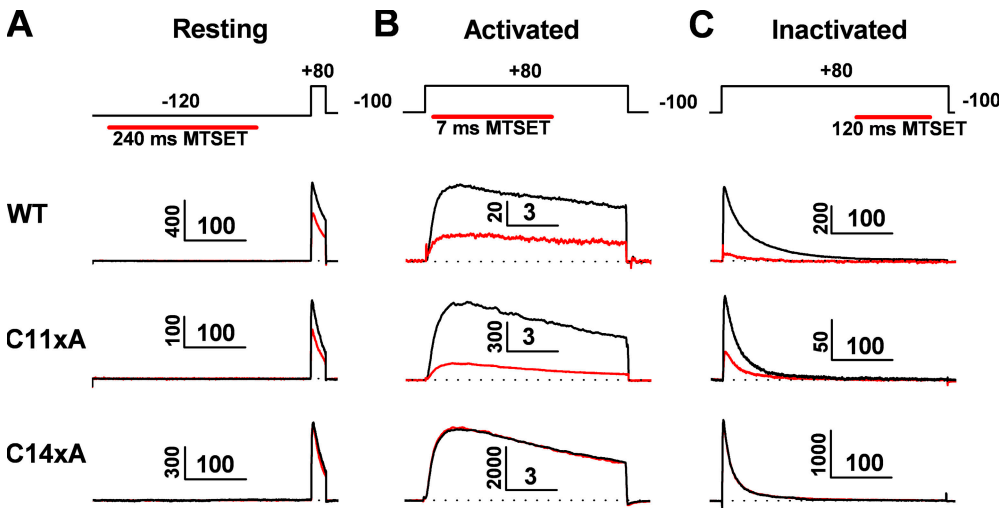

Figure 1. The T1 zinc binding site is accessible to internal MTSET in three distinct states. All channels were coexpressed with DPPX-S and KChIP-1. Wild-type (WT), C11xA, and C14xA currents from inside-out patches before (black) and after (red) the application of internal MTSET in the resting (left), activated (center), or inactivated (right) states. The units of current and time are pA and ms, respectively. Top, synchronized application of voltage steps (black line) and MTSET concentration jumps (red bar). The MTSET concentration was 200 μM for the activated state and 400 μM for the resting and inactivated states. The inhibition by MTSET during the test pulse is not apparent because the chemical modification and the resulting inhibition were slow relative to channel gating.

determining the magnitude of k_{MTSET} or its state dependence, we examined the ternary complexes of C12xA and C13xA. The coexpression of these mutants with KChIP1 and DPPX-S is necessary to rescue the lethal phenotype induced by the mutations of the Zn^{2+} cysteines (Wang et al., 2005; Kunjilwar et al., 2004) (MATERIALS AND METHODS). C12xA has two intracellular cysteines (C131 and C132) in the Zn^{2+} site, which cannot form an intersubunit metal bridge but an intrasubunit metal bridge with H104 (Nanao et al., 2003). By contrast, C13xA with only one intracellular cysteine in the Zn^{2+} site (C110) could form a relatively weak metal bridge between C110 and H104 (Nanao et al., 2003). Inhibition of both mutant channels by MTSET was state dependent in a manner qualitatively similar to that observed with C11xA (Table I). From the three mutants, C11xA, C12xA, and C13xA, the average difference between the k_{MTSET} of the activated and resting states was ~260-fold, and between activated and inactivated states was ~47-fold. Therefore, the integrity of the Zn^{2+} site is not necessary to preserve the state dependence of k_{MTSET}. Moreover, k_{MTSET} of the activated state increased proportionally with the number of cysteines in the T1 Zn^{2+} site (Fig. 3 and Fig. 6, A and B). Our previous studies showed that Kv4.1 mutants with their Zn^{2+} site either intact (C11xA) or disrupted (C12xA, C13xA, and C14xA) exhibit similar gating properties under the same condition (Wang et al., 2005). Thus, the relationship between k_{MTSET} and the number of Zn^{2+} site cysteines is unlikely to result from global channel distortions caused by the mutations. Instead, k_{MTSET} is simply a function of the number of potential targets/subunit, with the most significant increase occurring when this number increases from 1/subunit to 2 or 3/subunit (Table I, Fig. 3, and Fig. 6, A and B).

Tight Correlation between the Chemical Modification of the T1–T1 interface and Voltage-dependent Activation

If the state dependence of k_{MTSET} originates from the voltage-dependent activation process of the Kv4.1 channel, we expect a close correlation between the peak conductance–voltage (G_{PEAK}-Vm) and the k_{MTSET}–voltage (k_{MTSET}-Vm) relations. To test this hypothesis, we examined the inhibition of the ternary C11xA complex by MTSET at various membrane potentials between −120 and +120 mV. We conducted these experiments as described above for the activated state (Fig. 1, middle) except for voltages between −80 and −50 mV, which are not sufficiently depolarized to induce significant current activation. In this voltage range, an 80-ms MTSET pulse was first applied during a 100-ms step depolarization to −80 or −50 mV; the membrane potential was then hyperpolarized for 240 ms at −100 mV to remove any inactivation induced by the first pulse, and lastly a 4-ms test pulse to +80 mV was applied to monitor the available current. Fig. 4 shows that inhibition by MTSET became more rapid with membrane depolarization and was well described as an exponential decay. Thus, k_{MTSET} is voltage dependent. The best-fit fourth-order Boltzmann function estimated a maximal k_{MTSET} on the order of 21 $mM^{-1}s^{-1}$ (Fig. 5 B). Furthermore, there is a close correlation between the G_{PEAK}-Vm and k_{MTSET}-Vm relations (Fig. 5 B), which suggests that the conformational change in the T1–T1 interface faithfully mirrors activation gating of the Kv4 channel. In that case, any factor that shifts the voltage dependence of activation gating should shift the voltage dependence of k_{MTSET} as well. We tested this prediction in two ways: (1) coexpression of C11xA with DPPX-S only to induce a leftward shift of the G_{PEAK}-Vm relation (unpublished data); and (2) exposure of the ternary complex of

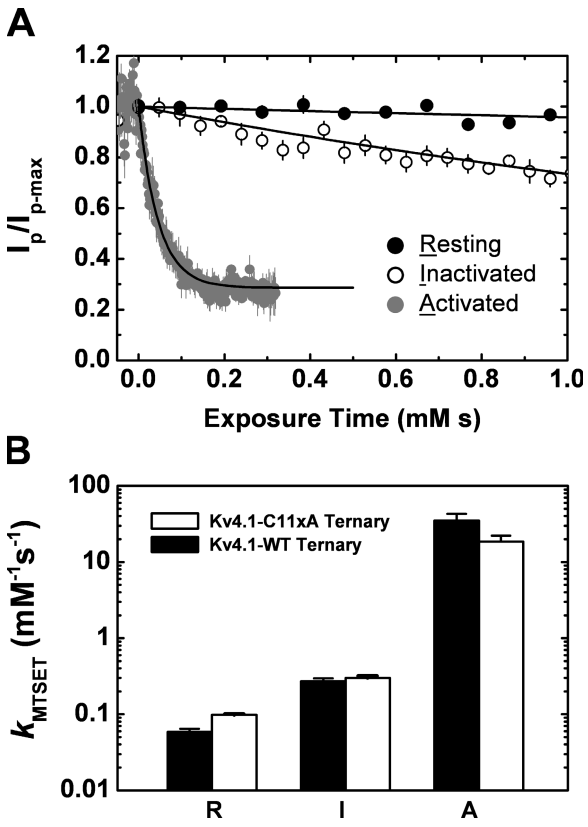

Figure 2. Gating state–dependent accessibility of the Kv4.1 channel T1–T1 interface to internal MTSET. (A) Time courses of C11xA ternary complex inhibition by internal MTSET in the activated (gray), inactivated (hollow circle), and resting (black) states. Solid lines are best-fit exponential decays with the following second-order rate constants ($1/\tau$[MTSET]): 0.038, 0.366, and 22 $mM^{-1}s^{-1}$ in the resting, inactivated, and activated states, respectively. The remaining fractional current at steady state was 0.2–0.25 in all states. (B) Bar graph summarizing the second-order rate constants of wild-type and C11xA ternary channel inhibition by MTSET.

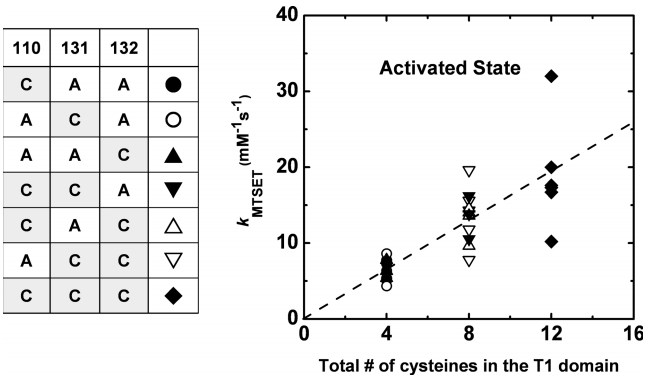

Figure 3. The k_{MTSET} in the activated state against the total number of cysteines in the T1 tetramer. The gray boxes (left) represent the available cysteines in the T1–T1 interface for different mutants. Mutants with one cysteine are variants of C13xA and those with two cysteines are variants of C12xA. The dashed line is the best-fit linear regression with a slope of 1.65 $mM^{-1}s^{-1}$/Cys.

C11xA to 400 μM Ni^{2+} (Cd^{2+} or Zn^{2+}) in the external pipette solution of the inside-out patch to induce a rightward shift of the G_{PEAK}-Vm relation (Song et al., 1998). We found indeed that the k_{MTSET}-Vm relation precisely followed the shifts induced by these two manipulations (Fig. 5). Therefore, the strong correlation between the voltage dependencies of G_{PEAK} and k_{MTSET} in three independent conditions is compelling evidence for a tight functional coupling between transmembrane voltage sensor and the intracellular T1–T1 intersubunit interface in a Kv channel during voltage-dependent gating.

Disulfide Bond Cross-linking Across the T1–T1 Interface Inhibits Kv4.1 Activation

If a movement of the T1–T1 interface is required for normal gating, locking the T1–T1 interface by forming a disulfide bond between two adjacent subunits should prevent the putative intersubunit displacement and thus suppress gating. Although the structure of the Zn^{2+}-free T1 site is not known, the available crystal structure of the T1 domain (Fig. 6, A and B) reveals that the distances between the β carbons of C110 and C131, C110 and C132, and C131 and C132 are 5.44 Å, 5.43 Å, and 3.97 Å, respectively. To form a disulfide bond, the β carbons of the cysteinyl groups in a rigid protein must be within 3.4–4.6 Å (Careaga and Falke, 1992); but in flexible proteins, the β carbons of the cysteinyl groups may be separated by as much as 15 Å (Falke and Koshland, 1987). Therefore, under proper conditions, the formation of intersubunit disulfide bonds in the channel tetramer is likely because our functional data suggest a dynamic T1–T1 interface. To test this hypothesis, we exposed the intracellular side of the channel to a mild oxidizing agent. Fig. 6 C shows that Cu/P (50 μM

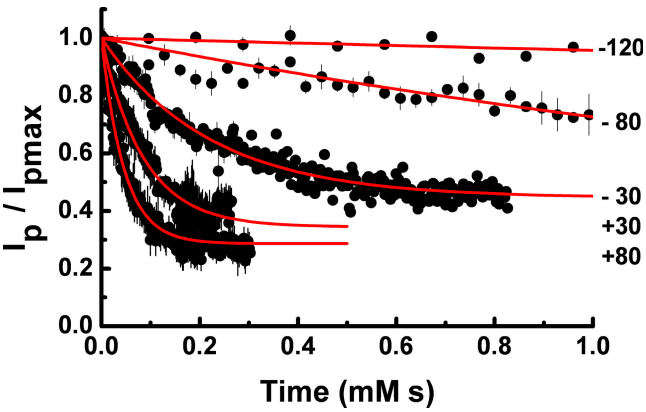

Figure 4. MTSET inhibition time courses of the Kv4.1-C11xA ternary complex at different membrane potentials. Solid lines are best-fit exponential decays with second-order rate constants ($1/\tau$[MTSET]) of 0.038, 0.42, 4.66, 11.77, and 21.93 $mM^{-1}s^{-1}$ at −120, −80, −30, +30, and +80 mV, respectively. MTSET concentrations are 200 μM above −30 mV and 400 μM below +30 mV.

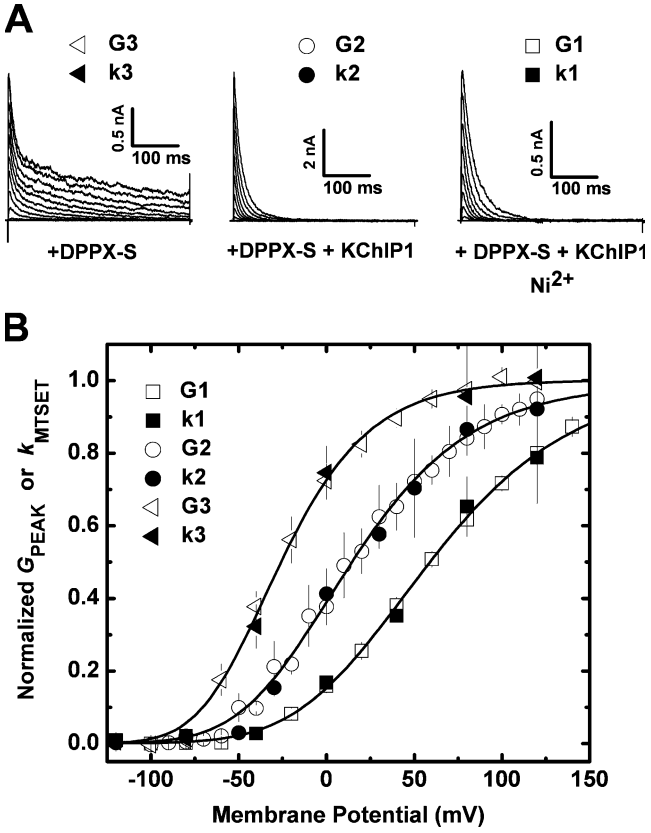

Figure 5. Voltage dependence of MTSET inhibition rate constants of the Kv4.1-C11xA channel. (A) Inside-out macropatch currents of Kv4.1-C11xA ternary, binary (+DPPX-S only), and ternary + Ni^{2+} (400 μM, external). Currents were evoked by step depolarizations from −100 mV to command voltages between −100 and +160 mV in 20-mV increments. (B) The k_{MTSET}-Vm (filled) and Gpeak-Vm (hollow) relations for the Kv4.1-C11xA channels depicted in A. The solid lines are the corresponding best-fit fourth-order Boltzmann functions with the following midpoint voltages ($V_{1/2}$) and slope factors (s): $V_{1/2}$ = −26 (binary), 14 (ternary), and 59 (ternary + Ni^{2+}); s = 32 (binary), 42 (ternary), and 51 (ternary + Ni^{2+}) mV. The maximal second-order rate constants ($mM^{-1}s^{-1}$) are 22.32 (binary), 21.13 (ternary), and 29.7 (ternary + Ni^{2+}), respectively. The k_{MTSET}-Vm and Gpeak-Vm relations in all three conditions are strongly correlated. The best-fit linear regression of a plot of all Gpeak-k_{MTSET} pairs has a slope = 1.002 and coefficient = 0.9954.

$CuSO_4$ and 200 μM phenanthroline; MATERIALS AND METHODS) inhibited the Kv4.1 current substantially when the intersubunit pair C110/C132 was available. Similarly, but to a lesser degree, inhibition was observed when the intersubunit pair C110/C131 was available. The inhibition was not reversible by washout of Cu/P, but the reducing agent DTT reversed it slowly (Fig. 7); and neither Cu^{2+} nor phenanthroline alone affected the Cu/P-sensitive mutants (unpublished data). In sharp contrast, when the intrasubunit pair C131/C132 or just C110 remained, there was no inhibition by Cu/P (Fig. 6 C). These observations suggest that the inhibition by Cu/P is not due to overoxidation of the thiolate to sufinic or sulfonic acid but to the formation of intersubunit disulfide bonds between C110 and C132 or between C110 and C131. Apparently, the latter pair formed the disulfide bond less efficiently than the former, suggesting that the spatial relationship between C110 and C132 is more favorable than between C110 and C131. To support this conclusion further, we investigated the inhibition by MTSET. If the cysteine pair forms a disulfide bond, the inhibition by MTSET would be reduced in a manner that reflects the efficiency of disulfide bond formation upon Cu/P treatment. Fig. 6 D shows that MTSET inhibited the currents by ∼76–79% when all T1 thiolate groups remained free. However, when the putative T1–T1 disulfide bonds were formed after pretreating with Cu/P, the mutant channels harboring the pairs C110/C132 and C110/C131 were inhibited by only ∼25% and 43%, respectively. These results showed that upon oxidation, fewer cysteines remained free and that disulfide bond formation was more efficient between C110 and C132, as hypothesized above. Altogether, the cross-linking results are consistent with channel inhibition resulting from strait-jacketing a functionally critical and dynamic T1–T1 interface during gating.

DISCUSSION

Others have established strong correlations between cysteine accessibility changes in the S4 or S6 transmembrane segments and gating charge movements or pore opening, respectively (Yang and Horn, 1995; Larsson et al., 1996; Yang et al., 1996; Liu et al., 1997; Baker et al., 1998; Mannikko et al., 2002). These correlations are the bases of the proposed mechanisms of activation gating in voltage-gated cation channels. Our results strongly suggest that the coupled conformational changes extend beyond the S4 and S6 segments into the interfacial Zn^{2+} site of the intracellular T1 domain in Kv4 channels.

Working Models and Mechanisms

From our earlier work and this study, we conclude that the Kv4 T1–T1 interface is functionally active because chemical modification of the Zn^{2+} site thiolate groups or intersubunit disulfide bridges involving these groups cause channel inhibition (Fig. 6) (Wang et al., 2005). This inhibition may result from a steric local perturbation or strait-jacketing of the T1 domain, respectively. In addition, we demonstrated that the cysteine accessibility is much faster in the activated state than in the resting or inactivated states (Fig. 3; Table I), and that k_{MTSET} is dependent on the membrane potential (Figs. 4 and 5). Importantly, this voltage dependence follows the Gp-V relation faithfully (Fig. 5). Thus, k_{MTSET} is tightly correlated with the channel's conductance change. Fig. 8 B illustrates hypothetical working models that attempts to explain these observations.

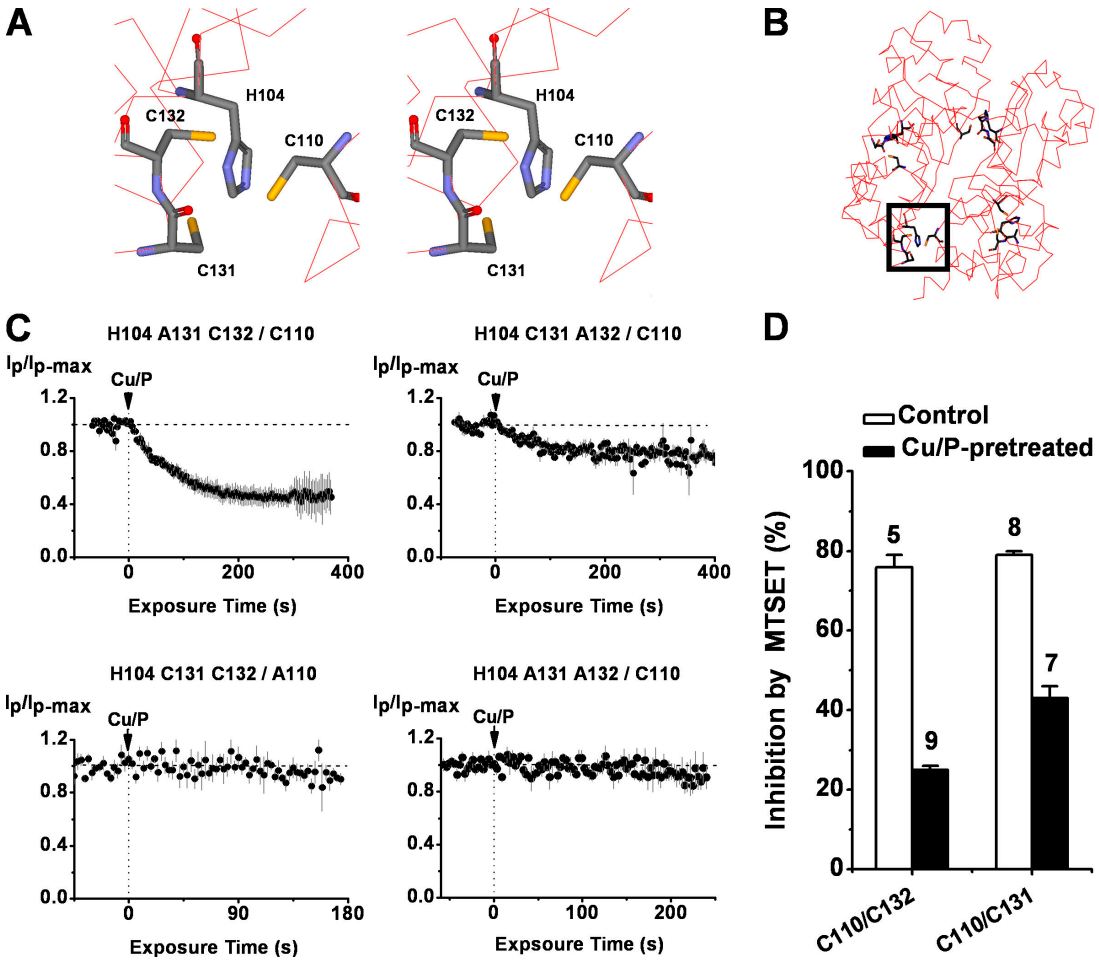

Figure 6. Disulfide bond cross-linking in the T1–T1 intersubunit interface inhibits ternary Kv4.1 channels. (A) Stereo view of the residues within the rectangle in B. C110 is from one subunit and C131, C132, and H104 are from the neighboring subunit. A standard color scheme is used to represent the relevant atoms. (B) Structural model of the Kv4 T1 domain. Colored sticks represent the residues that coordinate Zn^{2+} in the crystal structure, and red lines represent the rest of the T1 protein. Relative to its central axis, the model is tilted to emphasize the angle of view for the residues outlined by the rectangle. (C) The inhibition of Kv4.1 mutants by internally applied Cu/P. The available cysteines are indicated above each graph. Each symbol and corresponding error bars are the mean ± SEM of at least four experiments. (D) Bar graph summarizing the percent inhibition by MTSET (400 μM) before (white) and after treatment with Cu/P (black). The number of experiments is indicated above each bar. After the pretreatment with Cu/P, the differential inhibition of the two mutants by MTSET is statistically significant ($P < 0.0001$).

To create this cartoon models, we used the 3D crystal structure of Kv1.2 in the open state as a template (Fig. 8 A). Kv1.2 and Kv4.1 are expected to share similar structural features. Note that the voltage-sensing domains (VS) are connected to the pore domain (P) via the S4–S5 linkers, and to the T1 domain via the S1–T1 linkers; and that the T1 domain sits just below the S6 segments (and the S6 tails; not depicted). The latter is critical because the S6 helix bundle at the internal mouth of the channels is the main gate that controls the opening of the pore. Given these general features, including a relatively restricted space between the membrane-spanning core of the channel and the T1 domain, we propose that the closed T1–T1 interface and the S6 tail (or post-S6 segment) bury the critical Zn^{2+} site cysteines in the resting state. Therefore, the cysteine accessibility to MTSET is low. When membrane depolarization activates the channel, two alternative hypotheses may explain the dramatic increase in cysteine accessibility at the T1 Zn^{2+} sites (Fig. 8 B). In one scenario, the voltage-dependent displacement of the S4 sensor in the VS domain moves the S4–S5 linker and allows the opening the S6 helix bundle (Lu et al., 2002; Tristani-Firouzi et al., 2002; Long et al., 2005b). The latter opens the pore and exposes the T1–T1 interface, which undergoes a quasi-simultaneous conformational change through a possible direct interaction between the post-S6 segment and the T1–T1 interface at the level of the L4 layer (Fig. 8 B, bottom pathway). Ultimately, these conformational changes expose the Zn^{2+} site cysteines and increase the accessibility to MTSET. The interaction between post-S6 and

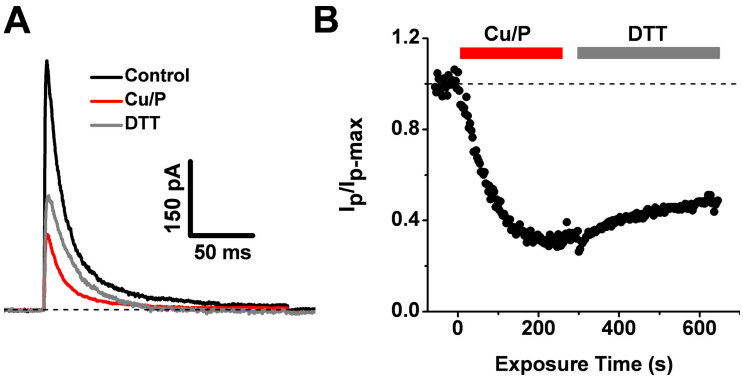

Figure 7. Reversibility of the Cu/P-induced inhibition of ternary Kv4.1 channels. (A) Outward currents evoked by a step depolarization from −100 to +80 mV. The currents were recorded in the inside-out configuration before (black trace) and after (red trace) the application of Cu/P to the intracellular side of the channels, and after exposing the same patch to 10 mM DTT (gray trace). The pH of the intracellular solution was 8.6 throughout the experiment. (B) The time course of the experiment shown in A. The currents in A are averages of ∼10 sweeps. From a total of three independent experiments, 32 ± 4% of the current inhibited by Cu/P was recovered upon the treatment with DTT.

the T1–T1 interface may be critical for the opening of the pore because T1–T1 cross-linking appeared to be sufficient to inhibit the channel. Also, because the S6 helix bundle is the main activation gate that controls the opening of the pore, the contributions of post-S6 help to explain the tight correlation between the voltage dependencies of k_{MTSET} and peak conductance. In the alternative scenario, the voltage-dependent displacement of the S4 segment moves the S4–S5 segment to open the pore and induces a rearrangement of the VS domain (Chanda et al., 2005), which propagates into the T1 domain via the S1–T1 linker. This propagated conformational change could open the T1–T1 interface locally at the Zn^{2+} site (L4 layer); however, to expose the cysteines and increase the accessibility to MTSET, the post-S6 segments would have to move too in a manner that is strictly coupled to the T1–T1 displacements. Therefore, if the T1–T1 interface cannot shift (e.g., upon intersubunit cross-linking), the S6 helix bundle cannot complete the pore opening. The VS domain-driven T1–T1 displacements alone cannot account for the observed voltage dependence of k_{MTSET} because this is tightly correlated with the Gp-V relation and the necessary movements of the voltage sensors (i.e., the Q-V relation) are expected to occur at more negative membrane potentials. Currently, our data cannot distinguish between these scenarios, and the mechanisms responsible for the inhibition are not known. Nevertheless, these working models provide concrete frameworks to investigate the striking voltage dependence of the putative conformational changes in the T1–T1 interface of Kv channels and their role in gating.

In contrast to the ∼260-fold change in cysteine accessibility between resting and activated channels, the average change is much smaller between resting and inactivated channels (∼3.7-fold) (Fig. 2; Table I). This observation may also be significant because it suggests that the closed and inactivated conformations of Kv4 channels are structurally alike, which is consistent with the presence of closed-state inactivation (Bahring et al., 2001; Beck and Covarrubias, 2001; Shahidullah and Covarrubias, 2003; Jerng et al., 2004). It is also in agreement with a model of closed-state inactivation induced by the decoupling between the S4 voltage sensor and the S6 gate (Shin et al., 2004). In this decoupled state, the resting and inactivated states of the channel may become functionally indistinguishable.

Physiological Significance

The proposed displacements could have important functional consequences. For instance, the T1–T1 interface may report the activation status of the channel. Consequently, the redox potential of the cell may modulate the functional activity of the T1–T1 interface in a state-dependent manner. A recent study has demonstrated acute state-dependent redox modulation of putative Kv4 channels in internally dialyzed cardiac myocytes and implicated intracellular sufhydryl groups (Rozanski and Xu, 2002). Based on our results, we propose that the Kv4 Zn^{2+} site cysteines are potential targets of physiological redox modulation in the heart. This modulation may exist in other excitable tissues and affect other Kv channels (Kv2 and Kv3), which also harbor the Zn^{2+} site cysteines in the T1 domain (Bixby et al., 1999).

At a more mechanistic level, the emerging multitasking picture of the T1 domain reveals three separate but fundamentally important functions: (1) T1 determines specific subunit coassembly within Kv subfamilies (Xu et al., 1995; Li et al., 1992; Bixby et al., 1999); (2) T1 is the anchoring site for auxiliary subunits of Kv channels (Gulbis et al., 2000; Scannevin et al., 2004; Callsen et al., 2005; Long et al., 2005a); and (3) in conjunction with the membrane spanning core and possibly other intracellular regions of the Kv channel, T1 contributes to the molecular rearrangements that govern gating. Perhaps the objective of this contribution is to allow the expansion of the lateral intracellular portals of the channel, which could favorably influence the opening of the main S6 gate and the rapid access of K^+ and the intracellular inactivation gate to the internal mouth of the Kv pore. This hypothetical expansion is reasonable because the lateral intracellular portals are clearly apparent

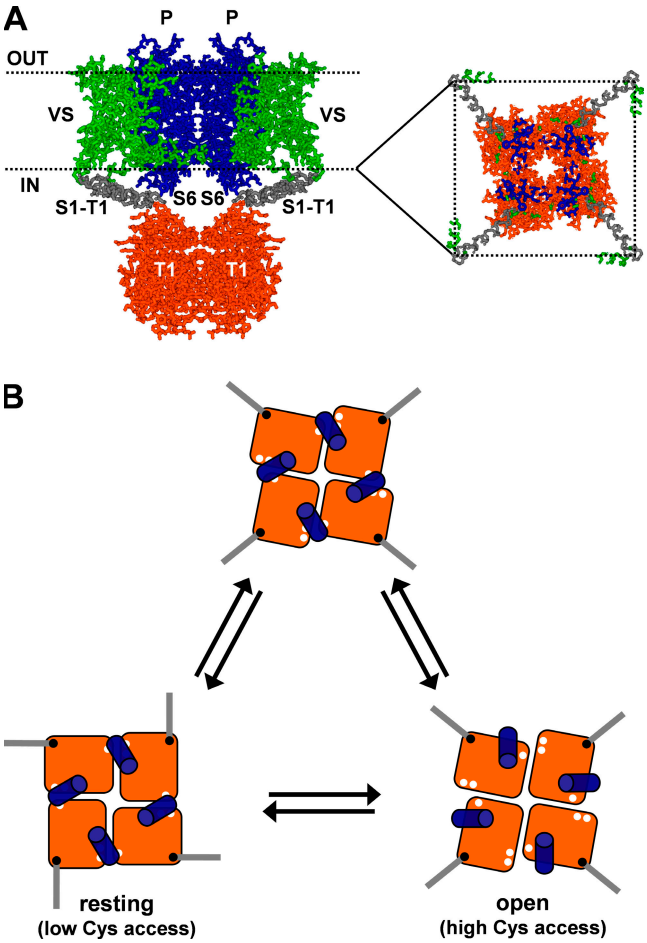

Figure 8. Coupling between voltage-dependent activation and the putative movements of the T1–T1 interfaces and the post-S6 segments. (A) Structural model of a Kv channel based on the 3D crystal structure of the Kv1.2 channel (Long et al., 2005a). The different colors depict distinct functional domains of the Kv channel: pore domain (P, blue), voltage sensing domain (VS, green; including the S4–S5 linker), and the T1 domain (T1, orange). The S1–T1 linkers (gray) connect the VS domain to the T1 domain. Dashed lines represent the approximate boundaries of the lipid bilayer. A section of the channel at the level of the internal boundary of the lipid bilayer is shown on the righthand side of the model. This view illustrates the fourfold symmetry of the channel oligomer with the S6-tails (blue) sitting just above the T1 domains and the S1–T1 linkers extending from each corner of the oligomer. (B) Two hypothetical pathways that explain the voltage dependence of the cysteine accessibility changes in the T1–T1 interface. The section shown in A (right) was used as a template to develop the schematic model of the T1 domain. The blue cylinders represent the post-S6 segments sitting on the T1–T1 interface when the pore is closed. At rest, the T1–T1 interfaces are buried. The upper pathway assumes VS domain-driven displacements of the T1–T1 interfaces via the S1–T1 linkers, which allow the concerted movement of the S6 helix bundle and the resulting opening of the pore. The lower pathway assumes the quasi-simultaneous displacements of the T1–T1 interfaces and the opening of the main S6 gate. In this case, exposing the T1–T1 interface does not depend on a propagated conformational change mediated by the S1–T1 linker. Instead, a direct interaction between the post-S6 segments and the L4 layers of T1 may drive the T1–T1 displacements as the S6 helix bundle expands to open the pore. In both pathways, the speculative conformational changes expose the Zn^{2+} site cysteines in a manner that reflects the increase in conductance resulting from the opening of the main activation gate.

between the membrane-spanning core and the T1 domain in the recently published crystal structure of a mammalian Kv channel in the open state (Kobertz et al., 2000; Kim et al., 2004; Long et al., 2005a).

Conclusion

We have provided compelling evidence for tight coupling between voltage-dependent activation of a Kv4 channel and conformational changes involving the intracellular T1–T1 interface. We propose that the complex structural rearrangements that control fast and efficient activation gating of eukaryotic Kv channels include propagated movements in the conserved L4 layer of the T1 domain and a post-S6 COOH-terminal segment that may contact the T1–T1 interface. These findings suggest novel ways to regulate Kv channel gating in excitable tissues.

We thank Dr. Mark Bowlby (Wyeth Research, Princeton, NJ) for providing KChIP-1 cDNA and Dr. Bernardo Rudy (New York University, New York, NY) for providing DPPX-S cDNA. We also thank Drs. Carol Deutsch, Paul De Weer, and Richard Horn for their critical reading of the manuscript.

This work was supported by United States Public Health Service (USPHS) research grant R01 NS32337 (M. Covarrubias) and in part by USPHS training grant T32 AA07463 (G. Wang).

Olaf S. Andersen served as editor.

Submitted: 21 October 2005
Accepted: 15 February 2006

REFERENCES

Bähring, R., L.M. Boland, A. Varghese, M. Gebauer, and O. Pongs. 2001. Kinetic analysis of open- and closed-state inactivation transitions in human Kv4.2 A-type potassium channels. *J. Physiol.* 535:65–81.

Baker, O.S., H.P. Larsson, L.M. Mannuzzu, and E.Y. Isacoff. 1998. Three transmembrane conformations and sequence-dependent displacement of the S4 domain in shaker K^+ channel gating. *Neuron.* 20:1283–1294.

Beck, E.J., and M. Covarrubias. 2001. Kv4 channels exhibit modulation of closed-state inactivation in inside-out patches. *Biophys. J.* 81:867–883.

Bezanilla, F., and E. Perozo. 2003. The voltage sensor and the gate in ion channels. *Adv. Protein Chem.* 63:211–241.

Bixby, K.A., M.H. Nanao, N.V. Shen, A. Kreusch, H. Bellamy, P.J. Pfaffinger, and S. Choe. 1999. Zn^{2+}-binding and molecular determinants of tetramerization in voltage-gated K^+ channels. *Nat. Struct. Biol.* 6:38–43.

Callsen, B., D. Isbrandt, K. Sauter, L.S. Hartmann, O. Pongs, and R. Bahring. 2005. Contribution of N- and C-terminal channel domains to Kv channel interacting proteins in a mammalian cell line. *J. Physiol.* 568:397–412.

Careaga, C.L., and J.J. Falke. 1992. Structure and dynamics of *Escherichia coli* chemosensory receptors. Engineered sulfhydryl studies. *Biophys. J.* 62:209–216.

Chanda, B., O.K. Asamoah, R. Blunck, B. Roux, and F. Bezanilla. 2005. Gating charge displacement in voltage-gated ion channels involves limited transmembrane movement. *Nature.* 436:852–856.

Cushman, S.J., M.H. Nanao, A.W. Jahng, D. DeRubeis, S. Choe, and P.J. Pfaffinger. 2000. Voltage dependent activation of potassium channels is coupled to T1 domain structure. *Nat. Struct. Biol.* 7:403–407.

Falke, J.J., and D.E. Koshland Jr. 1987. Global flexibility in a sensory receptor: a site-directed cross-linking approach. *Science.* 237:1596–1600.

Gulbis, J.M., M. Zhou, S. Mann, and R. MacKinnon. 2000. Structure of the cytoplasmic β subunit-T1 assembly of voltage-dependent K^+ channels. *Science.* 289:123–127.

Horn, R. 2000. Conversation between voltage sensors and gates of ion channels. *Biochemistry.* 39:15653–15658.

Jerng, H.H., P.J. Pfaffinger, and M. Covarrubias. 2004. Molecular physiology and modulation of somatodendritic A-type potassium channels. *Mol. Cell. Neurosci.* 27:343–369.

Karlin, A., and M.H. Akabas. 1998. Substituted-cysteine accessibility method. *Methods Enzymol.* 293:123–145.

Kim, L.A., J. Furst, D. Gutierrez, M.H. Butler, S. Xu, S.A. Goldstein, and N. Grigorieff. 2004. Three-dimensional structure of I(to); Kv4.2-KChIP2 ion channels by electron microscopy at 21 Å resolution. *Neuron.* 41:513–519.

Kobertz, W.R., C. Williams, and C. Miller. 2000. Hanging gondola structure of the T1 domain in a voltage-gated K^+ channel. *Biochemistry.* 39:10347–10352.

Kunjilwar, K., C. Strang, D. DeRubeis, and P.J. Pfaffinger. 2004. KChIP3 rescues the functional expression of Shal channel tetramerization mutants. *J. Biol. Chem.* 279:54542–54551.

Larsson, H.P., O.S. Baker, D.S. Dhillon, and E.Y. Isacoff. 1996. Transmembrane movement of the shaker K^+ channel S4. *Neuron.* 16:387–397.

Li, M., Y.N. Jan, and L.Y. Jan. 1992. Specification of subunit assembly by the hydrophilic amino-terminal domain of the Shaker potassium channel. *Science.* 257:1225–1230.

Liu, Y., M. Holmgren, M.E. Jurman, and G. Yellen. 1997. Gated access to the pore of a voltage-dependent K^+ channel. *Neuron.* 19:175–184.

Liu, Y., M.E. Jurman, and G. Yellen. 1996. Dynamic rearrangement of the outer mouth of a K^+ channel during gating. *Neuron.* 16:859–867.

Long, S.B., E.B. Campbell, and R. MacKinnon. 2005a. Crystal structure of a mammalian voltage-dependent shaker family K^+ channel. *Science.* 309:897–902.

Long, S.B., E.B. Campbell, and R. MacKinnon. 2005b. Voltage sensor of Kv1.2: structural basis of electromechanical coupling. *Science.* 309:903–908.

Lu, Z., A.M. Klem, and Y. Ramu. 2002. Coupling between voltage sensors and activation gate in voltage-gated K^+ channels. *J. Gen. Physiol.* 120:663–676.

Mannikko, R., F. Elinder, and H.P. Larsson. 2002. Voltage-sensing mechanism is conserved among ion channels gated by opposite voltages. *Nature.* 419:837–841.

Minor, D.L., Y.F. Lin, B.C. Mobley, A. Avelar, Y.N. Jan, L.Y. Jan, and J.M. Berger. 2000. The polar T1 interface is linked to conformational changes that open the voltage-gated potassium channel. *Cell.* 102:657–670.

Nanao, M.H., W. Zhou, P.J. Pfaffinger, and S. Choe. 2003. Determining the basis of channel-tetramerization specificity by x-ray crystallography and a sequence-comparison algorithm: family values (FamVal). *Proc. Natl. Acad. Sci. USA.* 100:8670–8675.

Robinson, J.M., and C. Deutsch. 2005. Coupled tertiary folding and oligomerization of the T1 domain of Kv channels. *Neuron.* 45:223–232.

Rozanski, G.J., and Z. Xu. 2002. Sulfhydryl modulation of K^+ channels in rat ventricular myocytes. *J. Mol. Cell. Cardiol.* 34:1623–1632.

Scannevin, R.H., K. Wang, F. Jow, J. Megules, D.C. Kopsco, W. Edris, K.C. Carroll, Q. Lu, W. Xu, Z. Xu, et al. 2004. Two N-terminal domains of Kv4 K^+ channels regulate binding to and modulation by KChIP1. *Neuron.* 41:587–598.

Shahidullah, M., and M. Covarrubias. 2003. The link between ion permeation and inactivation gating of Kv4 potassium channels. *Biophys. J.* 84:928–941.

Shin, K.S., C. Maertens, C. Proenza, B.S. Rothberg, and G. Yellen. 2004. Inactivation in HCN channels results from reclosure of the activation gate: desensitization to voltage. *Neuron.* 41:737–744.

Song, W.J., T. Tkatch, G. Baranauskas, N. Ichinohe, S.T. Kitai, and D.J. Surmeier. 1998. Somatodendritic depolarization-activated potassium currents in rat neostriatal cholinergic interneurons are predominantly of the A type and attributable to coexpression of Kv4.2 and Kv4.1 subunits. *J. Neurosci.* 18:3124–3137.

Tristani-Firouzi, M., J. Chen, and M.C. Sanguinetti. 2002. Interactions between S4-S5 linker and S6 transmembrane domain modulate gating of HERG K^+ channels. *J. Biol. Chem.* 277:18994–19000.

Wang, G., M. Shahidullah, C.A. Rocha, C. Strang, P.J. Pfaffinger, and M. Covarrubias. 2005. Functionally active T1-T1 interfaces revealed by the accessibility of intracellular thiolate groups in kv4 channels. *J. Gen. Physiol.* 126:55–69.

Xu, J., W. Yu, Y.N. Jan, L.Y. Jan, and M. Li. 1995. Assembly of voltage-gated potassium channels. Conserved hydrophilic motifs determine subfamily-specific interactions between the α-subunits. *J. Biol. Chem.* 270:24761–24768.

Yang, N., A.L. George Jr., and R. Horn. 1996. Molecular basis of charge movement in voltage-gated sodium channels. *Neuron.* 16:113–122.

Yang, N., and R. Horn. 1995. Evidence for voltage-dependent S4 movement in sodium channels. *Neuron.* 15:213–218.

Yellen, G. 1998. The moving parts of voltage-gated ion channels. *Q. Rev. Biophys.* 31:239–295.